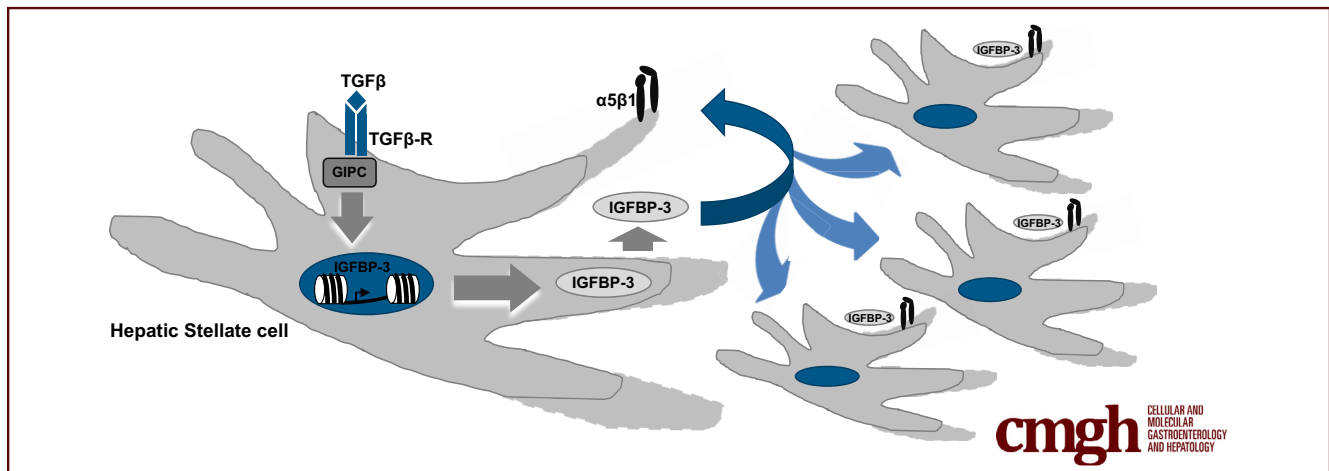


ORIGINAL RESEARCH

GIPC-Regulated IGFBP-3 Promotes HSC Migration In Vitro and Portal Hypertension In Vivo Through a $\beta 1$ -Integrin Pathway

Usman Yaqoob,^{1,*} Fanghong Luo,^{1,2,*} Thomas Greuter,^{1,3} Nidhi Jalan Sakrikar,¹ Tejasav S. Sehrawat,¹ Jianwen Lu,¹ Xiao Hu,¹ Jinhang Gao,¹ Enis Kostallari,¹ Jingbiao Chen,¹ Juan Pablo Arab,¹ Rosa Martin-Mateos,^{1,4} Sheng Cao,^{1,*} and Vijay H. Shah¹

¹Gastroenterology Research Unit, Division of Gastroenterology and Hepatology, Mayo Clinic, Rochester, Minnesota; ²Cancer Research Center, Medical College, Xiamen University, Xiamen, China; ³Division of Gastroenterology and Hepatology, University Hospital Zurich, Zurich, Switzerland; ⁴Division of Gastroenterology and Hepatology, Ramón y Cajal University Hospital, Madrid, Spain



SUMMARY

Insulin-like growth factor binding protein-3 is a transforming growth factor- β -responsive gene that is regulated transcriptionally by GAIIP interacting protein C-terminus. It promotes hepatic stellate cell migration through integrin and protein kinase B dependent pathway leading to portal hypertension in vivo.

BACKGROUND & AIMS: Transforming growth factor (TGF- β)-induced activation of quiescent hepatic stellate cells (HSCs) and their transformation to myofibroblasts is a key event in liver fibrosis and portal hypertension. GIPC (also referred to as synectin) is a downstream signal activation molecule of TGF- β and other receptors. In this study, we sought to identify novel genes targeted by TGF- β and GIPC and elucidate if and how they may contribute to liver fibrosis.

METHODS: We performed sequential messenger RNA sequencing analysis on TGF- β -stimulated HSCs and then on TGF- β -stimulated HSCs in the presence and absence of GIPC also referred to as synectin (GIPC) knockdown. Insulin-like growth factor binding protein-3 (IGFBP-3) transport protein emerged as a top activation target of both TGF- β and GIPC. Quantitative polymerase chain reaction, enzyme-linked immunosorbent assay, targeted chromatin immunoprecipitation, and Western blot analysis were done for further confirmation.

RESULTS: IGFBP-3, an insulin growth factor transport protein, emerged as a top activation target of both TGF- β and GIPC, which was confirmed by quantitative polymerase chain reaction, enzyme-linked immunosorbent assay, and Western blot analysis. Targeted chromatin immunoprecipitation showed that GIPC increases the histone 3 lysine 27 (H3K27) acetylation activating mark and concurrently decreases the H3K27 inhibitory trimethylation (H3K27m3) mark, providing an epigenetic correlate to the gene regulation changes. In vivo, global knockout of IGFBP-3 mice resulted in attenuation of HSC activation markers and attenuation of portal pressure in response to chronic liver injury models. Analysis of serum levels from cirrhotic patients also showed an IGFBP-3 increase of more than 2-fold compared with healthy controls. Finally, in vitro mechanism studies showed that IGFBP-3 promotes HSC migration through integrin-dependent phosphorylation of protein kinase B.

CONCLUSIONS: TGF- β up-regulates IGFBP-3 through GIPC, leading to increased HSC migration in vitro and promotes portal hypertension in vivo. These studies support the role of IGFBP-3 as a potential pathophysiologic target or biomarker in chronic liver disease. (*Cell Mol Gastroenterol Hepatol* 2020;10:545-559; <https://doi.org/10.1016/j.jcmgh.2020.05.005>)

Keywords: Fibrosis; Hepatic Stellate Cells; IGFBP-3; Integrin Signaling; Liver; Migration; GIPC.

Hepatic stellate cells (HSCs) drive liver fibrosis via their activation into myofibroblasts, which are contractile, proliferative, motile, and deposit extracellular matrix.^{1,2} Molecules involved in HSC activation such as transforming growth factor- β (TGF- β) and its corresponding receptors³ have been studied extensively, but exact mechanisms still remain only partially understood, which has hindered appropriate drug development.⁴⁻⁶ This study and other previous studies have shown that GIPC is a scaffold protein that regulates transmembrane-receptor signaling including TGF- β receptor.⁷ As a downstream signaling molecule, GIPC plays an important role in signaling transduction.⁸ Our understanding on how TGF activates HSC through GIPC and novel targets is a gap in knowledge and a focus of our current study.

Insulin-like growth factor binding protein 3 (IGFBP-3) is 1 of the 6 known IGFBPs.⁹ The liver is one of the major sources of circulating IGFBP-3, which shows growth-inhibitory properties by blocking interaction between IGF1/2 and its receptor.^{10,11} IGFBP-3 also has been shown to affect cell function by IGF-receptor-independent signaling pathways.¹²⁻¹⁵ Furthermore, IGFBP-3 is implicated in HSC activation based on gene expression profiling studies from quiescent and activated HSCs.¹⁶ Inhibition of HSC activation has been shown to prevent IGFBP-3 transcription in vitro and in vivo.¹⁶ However, additional information pertaining to IGFBP-3 and liver fibrosis beyond this correlative information is not available.

To explore liver fibrosis targets downstream of TGF- β and GIPC in a nonbiased manner, we performed sequential RNA sequencing studies. Our initial messenger RNA (mRNA) sequencing analysis of TGF- β in HSCs identified IGFBP-3 as one of the top downstream targets. Furthermore, in our second mRNA sequencing screening, IGFBP-3 was identified further as one of the top targets of GIPC. Based on this information we further explored the following: (1) the mechanism by which TGF- β and GIPC activate IGFBP-3 gene transcription, (2) effects of IGFBP-3 on liver fibrosis in vivo, and (3) mechanisms of effect of IGFBP-3 on HSCs in vitro. We show that GIPC knockdown decreases TGF- β -induced IGFBP-3 expression through epigenetic modifications of histone 3 lysine K27 (H3K27) within the IGFBP-3 promoter. Global knockdown of IGFBP-3 attenuates portal hypertension and liver fibrosis in the bile duct ligation (BDL) and carbon tetrachloride (CCl₄) murine models. Moreover, IGFBP-3 levels in the serum from patients with cirrhotic livers are significantly higher than levels from normal livers. Finally, IGFBP-3 promotes HSC activation through an integrin-Protein Kinase B (AKT) signaling pathway. Our findings show a novel mechanism of HSC regulation mediated by IGFBP-3, and may provide a potential therapeutic target in the treatment of liver fibrogenesis and portal hypertension.

Results

RNA Sequencing Identifies a Gene Network in HSCs That Includes IGFBP-3 as an Important Target Gene of TGF- β

TGF- β is one of the most potent promoters for HSC activation. However, mechanisms of this activation only partially

are understood. To evaluate novel downstream targets of TGF- β signaling, we performed mRNA sequencing analysis of HSC stimulated with TGF- β for 48 hours compared with nonstimulated HSCs (Figure 1A). Ingenuity pathway analysis of the top up-regulated and down-regulated genes showed hepatic fibrosis/hepatic stellate cell activation as the top signaling pathway based on $-\log P$ values (Figure 1B). Unexpectedly, using this nonbiased approach, we identified IGFBP-3 as one of the top targets of TGF- β within the hepatic fibrosis pathway alongside the expected canonical TGF- β -induced genes for collagen (COL8A1, COL7A1, COL5A1, COL4A2, COL4A1, COL3A1, COL1A1, and COL16A1), α -smooth muscle actin 2, and fibronectin (Figure 1C). The increase of IGFBP-3 in both cell lysates and culture media was confirmed by Western blot (WB) (Figure 1D). This RNA sequencing data pointed us toward IGFBP-3 as a target warranting further interrogation.

IGFBP-3 Up-regulation in Response to TGF- β Is Dependent on the Scaffold Protein GIPC


Recently, our group identified the scaffold protein GIPC as an important molecule in membrane-receptor signaling and HSC activation.⁷ To investigate the role of GIPC as a possible regulator of TGF- β -induced IGFBP-3 expression in HSCs, we performed a second mRNA sequencing analysis of HSCs with a knockdown of GIPC vs controls stimulated with TGF- β as early as 2 hours (Figure 2A). By using ingenuity pathway analysis, again we identified hepatic fibrosis/hepatic stellate cell activation as the top signaling pathway blocked by GIPC knockdown (Figure 2B). Within this pathway, IGFBP-3 also was identified as one of the top targets of GIPC alongside α -smooth muscle actin 2, collagen (COL11A2, COL15A1, COL4A1, COL5A3), platelet-derived growth factor receptors α and β (PDGFR α and β), PDGFRD, and serpine1 (Figure 2C). Given the novelty of IGFBP-3 compared with other well-characterized fibrogenic proteins identified from sequencing, we subsequently focused our mechanistic studies on IGFBP-3.

IGFBP-3 Is Expressed Predominantly in HSCs

Because IGFBP-3 is a secreted protein, we first identified the cellular source of IGFBP-3 in the liver. HSCs emerged as the top liver cell type with increased IGFBP-3 expression via

*Authors share co-first authorship.

Abbreviations used in this paper: α SMA, α -smooth muscle actin; AKT, Protein Kinase B; BDL, bile duct ligation; bp, base pair; CCl₄, carbon tetrachloride; ChIP, chromatin-immunoprecipitation; chr, chromosome; ELISA, enzyme-linked immunosorbent assay; EZH, enhancer of zeste homologue; GAPDH, glyceraldehyde-3-phosphate dehydrogenase; hg, human genome browser; IGFBP-3, insulin-like growth factor binding protein-3; HSC, hepatic stellate cell; H3K27, histone 3 lysine K27; LSEC, liver sinusoidal endothelial cells; mRNA, messenger RNA; PDGFR, platelet-derived growth factor receptor; qPCR, quantitative polymerase chain reaction; siRNA, small interfering RNA; TGF- β , transforming growth factor β ; WB, Western blot; WT, wild-type.

 Most current article

© 2020 The Authors. Published by Elsevier Inc. on behalf of the AGA Institute. This is an open access article under the CC BY-NC-ND license (<http://creativecommons.org/licenses/by-nc-nd/4.0/>).

2352-345X

<https://doi.org/10.1016/j.jcmgh.2020.05.005>

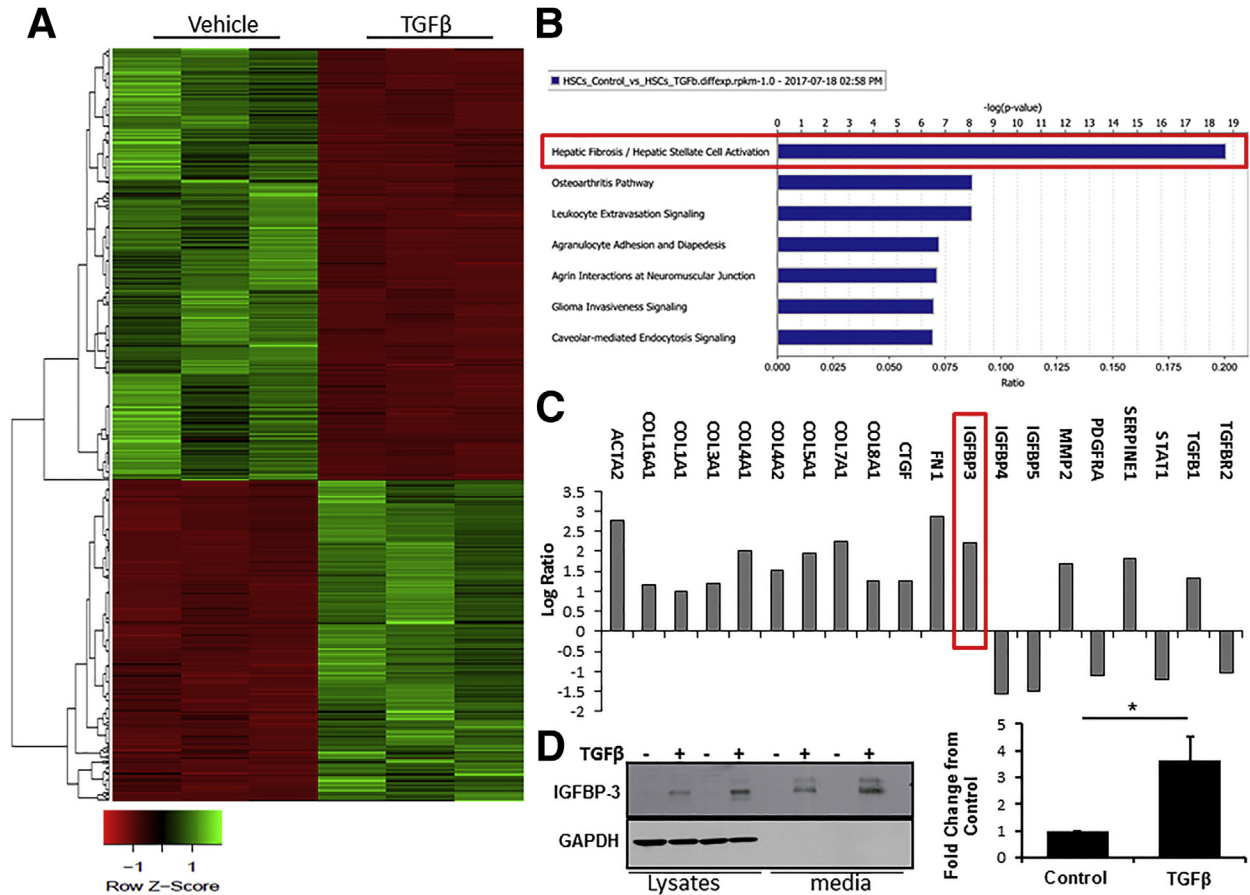


Figure 1. The hepatic fibrosis/HSC activation pathway is the most highly regulated pathway by TGF- β treatment through transcriptomic analysis. (A) Cultured human HSCs (hHSCs) were serum-starved overnight and treated with vehicle and TGF- β . Cells were harvested and mRNA was collected and samples were submitted to NextGen (Mayo Clinic, Rochester, MN) sequencing core for library preparation and sequencing after an initial quality-control check. A heat map of whole-genome gene expression shows the differences in the expression profile between vehicle- and TGF- β -treated hHSCs, which were run in triplicate, of all genes with a log fold change > 1.5 and < -1.5 . (B and C) Ingenuity pathway analyses (Qiagen) showed that the fibrotic pathway was regulated differentially between the groups. Regulation of specific genes within the hepatic fibrosis/HSC activation pathway are shown, with IGFBP-3 highlighted in the red outlined rectangles. (D) Immunoblot of IGFBP-3 from hHSCs serum-starved overnight and treated with TGF- β for 48 hours showed an increase in the production of IGFBP-3. Both cell lysates and conditioned media were collected to detect IGFBP-3 (cellular and secreted proteins are shown in duplicate). GAPDH was used as a loading control. Results are from 3 independent experiments. The Student unpaired, 2-tailed t test was used to analyze the differences between groups for statistical significance. * $P < .05$. diffexp, differential expression; rpkM, Million mapped reads.

quantitative polymerase chain reaction (qPCR) analysis (Figure 3A). Single-cell RNA sequencing analysis from mouse liver from olive oil or CCl₄ treatment showed clusters of nonparenchymal liver cells with enhanced IGFBP-3 expression along with other HSC marker genes such as COL1A1 and PDGFR β in the same cluster 10 (Figure 3B and C), suggesting that IGFBP-3 is expressed mainly in HSCs in both basal and CCl₄ activation conditions.

IGFBP-3 Expression and Release Is Decreased Both In Vitro and In Vivo After GIPC Knockdown

To establish and investigate the relationship between GIPC and IGFBP-3, we sought to explore further the effects of GIPC knockdown and to confirm the results found in the RNA sequencing analysis. By using qPCR, enzyme-linked

immunosorbent assay (ELISA) and WB, we detected a significant down-regulation of both IGFBP-3 mRNA and protein levels in HSCs after GIPC knockdown (Figure 4A and B). Furthermore, decreased IGFBP-3 levels in the cell media indicated a reduced protein release after GIPC knockdown (Figure 4C). To study the effect of GIPC knockdown on IGFBP-3 in vivo, we used mice carrying floxed GIPC alleles, which were crossed with animals that express Cre under the COL1A1 promoter, which generated mouse lines with HSC-selective deletion of GIPC (referred to as Col^{cre}/GIPC^{fl/fl}). Prior studies showed that these mice developed attenuation of liver fibrosis in response to chronic CCl₄ administration.⁷ Herein, we clearly found a significant reduction in IGFBP-3 release to the serum (Figure 4D). Both hepatic IGFBP-3 mRNA and protein levels were decreased in Col^{cre}/GIPC^{fl/fl} mice compared with controls. Taken together, these

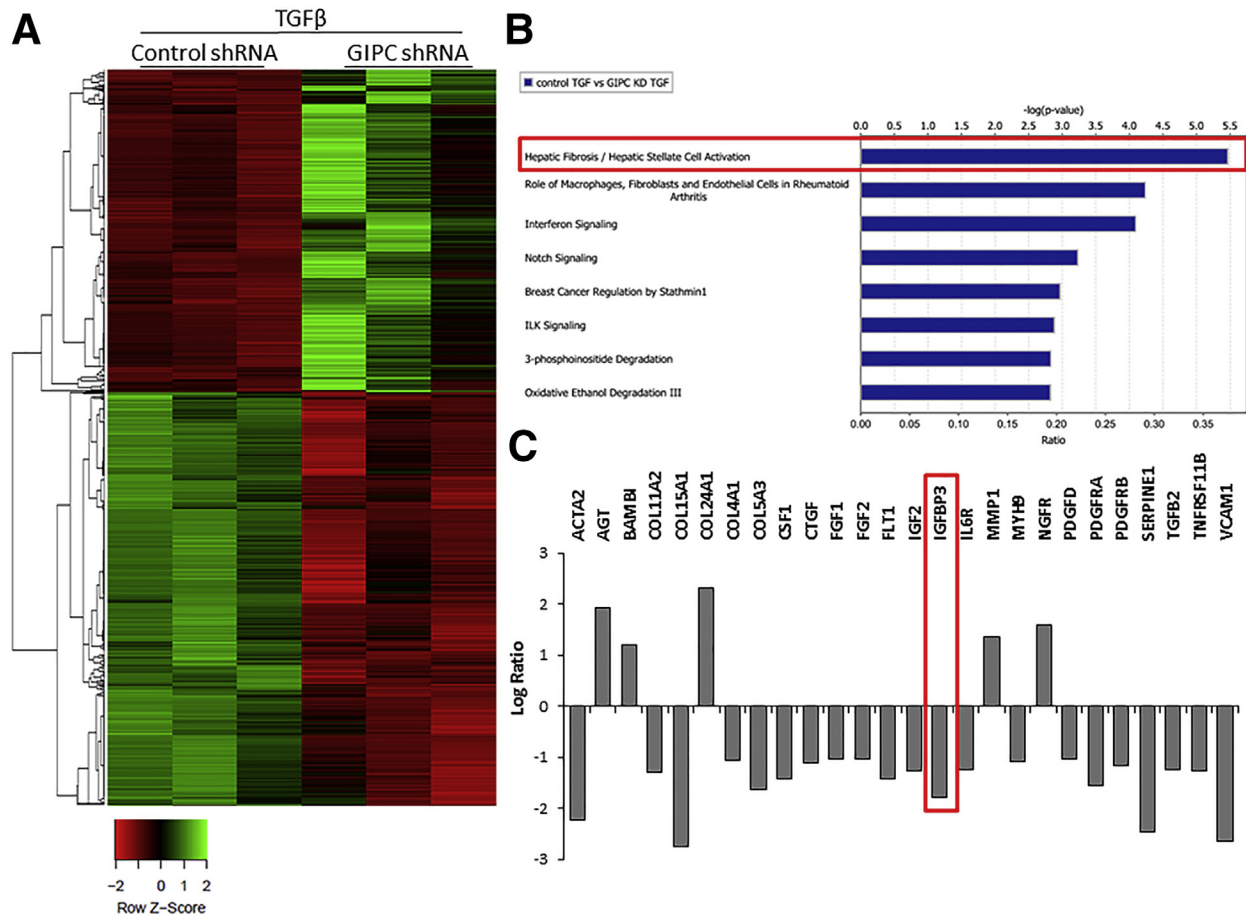


Figure 2. The hepatic fibrosis/HSC activation pathway is the most highly regulated pathway by GIPC knock down in HSCs. (A) GIPC was knocked down in cultured human HSCs using lentiviral-mediated short hairpin RNA. Cells were serum-starved overnight and treated with vehicle and TGF- β for 2 hours. mRNA was collected and samples were submitted to NextGen sequencing core (Mayo Clinic, Rochester, MN) for library preparation and sequencing. Differences in the expression profile between control and GIPC knockdown human HSCs with TGF- β treatment are shown in the heat map of whole-genome gene expression. Samples were run in triplicate, of all genes with a logFc > 1.5 of < -1.5. (B and C) Ingenuity pathway analyses (Qiagen) showed that the HSC activation/fibrotic pathway was regulated differentially by GIPC. Regulation of specific genes within the hepatic fibrosis/HSC activation pathway are shown. Top pathway and IGFBP3 are highlighted in the red outlined rectangles. KD, knockdown; ILK, integrin-linked kinase.

experiments showed that GIPC promotes IGFBP-3 production and release.

IGFBP-3 Expression Is Regulated by GIPC Through H3K27 Acetylation and Methylation of the IGFBP-3 Promoter

Gene expression is regulated commonly by P300 and histone modification at lysine 27 acetylation (H3K27Ac, leading to gene activation), and histone trimethylation at lysine 27 (H3K27me3), resulting in gene repression by enhancer of zeste homologue 2 (EZH2).¹⁷ Studies with human melanoma and hepatocellular carcinoma cell lines have further implicated a role for histone acetylation in IGFBP-3 expression.^{18–21} Our investigation of the ENCODE TFBS database (encode.org) suggested that there are 2 overlapping EZH2 binding sites in the human IGFBP-3 transcription start site region (human genome browser [hg19], chromosome 7 [chr7]:45959379-45960659/chr7:45959718-45961110), and another at the promoter

region (hg19 chr7:45961121-45962023). Based on this rationale, we designed primers to pursue chromatin-immunoprecipitation (ChIP) experiments in primary human HSC with a lentiviral-based knockdown of GIPC and IGFBP-3–promoter luciferase assays to explore the relationship of GIPC with the inhibitory H3K27me3 epigenetic mark on the IGFBP-3 gene locus and IGFBP-3 transcription activity, respectively. ChIP analysis showed that knockdown of GIPC increased H3K27me3 repression marks on the IGFBP-3 gene locus while decreasing H3K27Ac (Figure 5A and B). Accordingly, nuclear protein expression of H3K27m3 increased, whereas that of H3K27Ac was reduced (Figure 5C). We further examined for H3K27Ac with a pharmacologic inhibitor. H3K27Ac inhibition was achieved with chemical inhibition using compound cAMP-responsive element binding protein binding protein30, which is a potent cAMP-responsive element binding protein binding protein/p300 (the major histone acetyltransferase to affect H3K27Ac level) BRD inhibitor.²² As

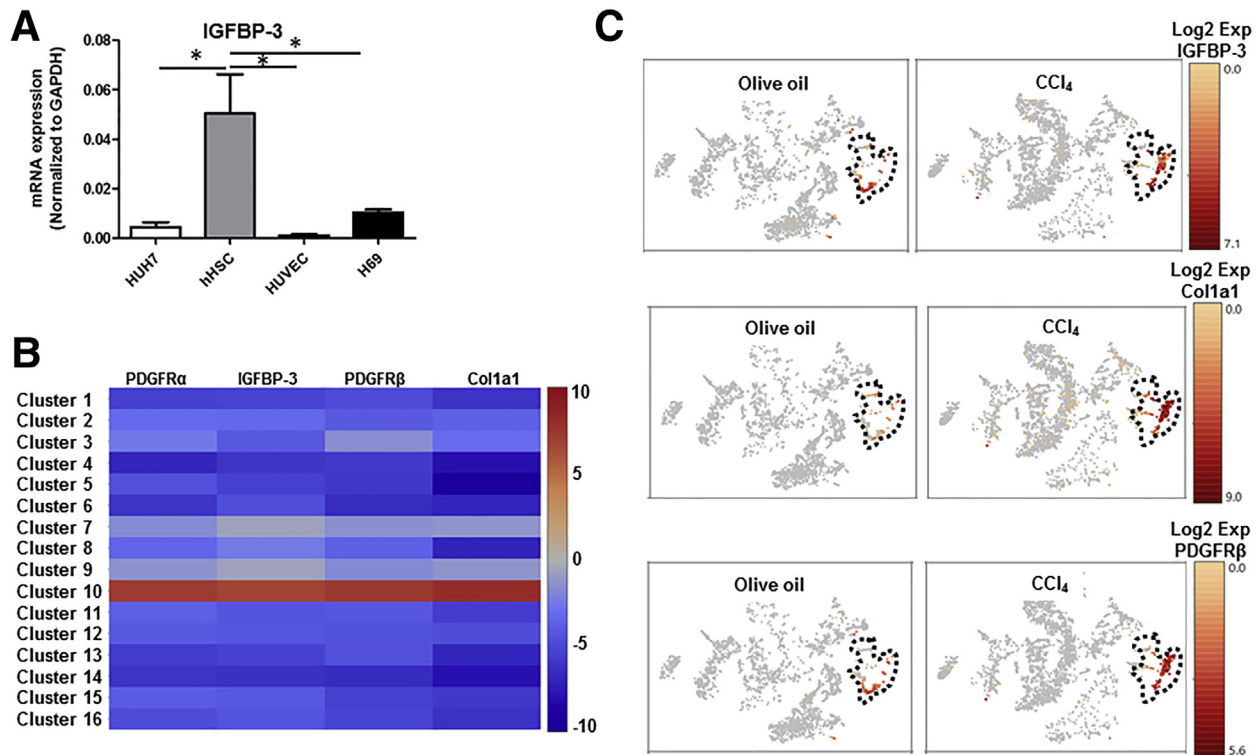


Figure 3. IGFBP-3 is expressed prominently in HSCs. (A) qPCR from various hepatic and nonhepatic cell lines shows higher mRNA levels of IGFBP-3 in human HSCs (hHSCs) compared with other cell lines. One-way analysis of variance with Bonferroni multiple comparison tests was used to analyze groups for statistical significance. $*P < .05$. (B) Heat map of HSC cluster marker genes labeled on the top from mouse liver cells undergo olive oil and CCl₄ treatment. Columns denote genes; rows denote clusters. (C) Clustering of cells from mouse liver treated with olive oil and CCl₄. Cluster 10 represents HSCs with a high expression of COL1A1, PDGFR β , and IGFBP-3. Exp, Exponent; HUH7, hepatocyte-derived carcinoma cell line; HUVEC, human umbilical vein endothelial cell; H69, human lung small-cell carcinoma cell line.

expected, TGF- β -induced IGFBP-3 mRNA levels in HSCs were reduced after p300 inhibition (Figure 5D). These results indicate that GIPC regulates IGFBP-3 transcription through H3K27m3 suppression and H3K27Ac activation.

Next, we aimed to investigate the effect of GIPC knockdown on luciferase-reporter activity. HSCs with GIPC knockdown showed a 90% reduction in promoter activity (Figure 5E). Next, we performed a promoter analysis using the following 2 IGFBP-3 promoter luciferase reporter plasmids: pGL3-IGFBP-3 full length (-3595 base pairs [bp] to +55 bp) and gGL3-IGFBP-3 deletion (-1950 bp to +55 bp), which were transfected into HSCs followed by luciferase assay.^{23,24} Luciferase activity of IGFBP-3 promoter full length and deletion showed similar down-regulation by GIPC knockdown, suggesting that +55 bp to -1950 bp of the IGFBP-3 transcription start site may contain an EZH2 binding motif and may be required for H3K27m3 repression induced by GIPC knockdown. Taken together, our data show that GIPC's effect on IGFBP-3 occurs through histone modification and transcriptional regulation on IGFBP-3 promoter.

Global Knockout of IGFBP-3 Attenuates HSC Activation In Vivo

Given the effects of IGFBP-3 on HSC activation and migration, we aimed to investigate if global knockout of IGFBP-3 results in attenuation of HSC activation markers

in vivo. For this purpose, we used mice with deletion of both alleles of the IGFBP-3 gene (referred to as IGFBP-3^{-/-}). BDL surgery was used to induce liver fibrosis. Portal pressure, Sirius red staining, hepatic collagen content, and α -smooth muscle actin (α SMA) were lower in IGFBP-3^{-/-} mice compared with genotype control mice 4 weeks after BDL surgery (Figure 6A–D). IGFBP-3 levels were increased in the serum of wild-type (WT) mice after BDL surgery (Figure 6E), but not in IGFBP-3^{-/-} mice. We next used CCl₄ as a second model of liver fibrosis. IGFBP-3^{-/-} mice showed attenuated up-regulation of SMA in response to CCl₄ compared with WT mice in response to CCl₄ (Figure 7A). Serum IGFBP-3 levels were increased in mice after CCl₄-induced liver fibrosis, but not in IGFBP-3^{-/-} mice (Figure 7B). Next, we isolated HSCs from WT and IGFBP-3^{-/-} mice. HSCs derived from IGFBP-3^{-/-} mice showed less culture-induced activation after 72 hours compared with WT mice as indicated by α SMA mRNA levels (Figure 7C). IGFBP-3 knockout was confirmed as well by qPCR (Figure 7D).

IGFBP-3 Expression Is Up-regulated in Patients With Alcoholic Cirrhosis

To gain insight into the role of IGFBP-3 in human cirrhosis, we analyzed serum and liver samples from 6 patients with

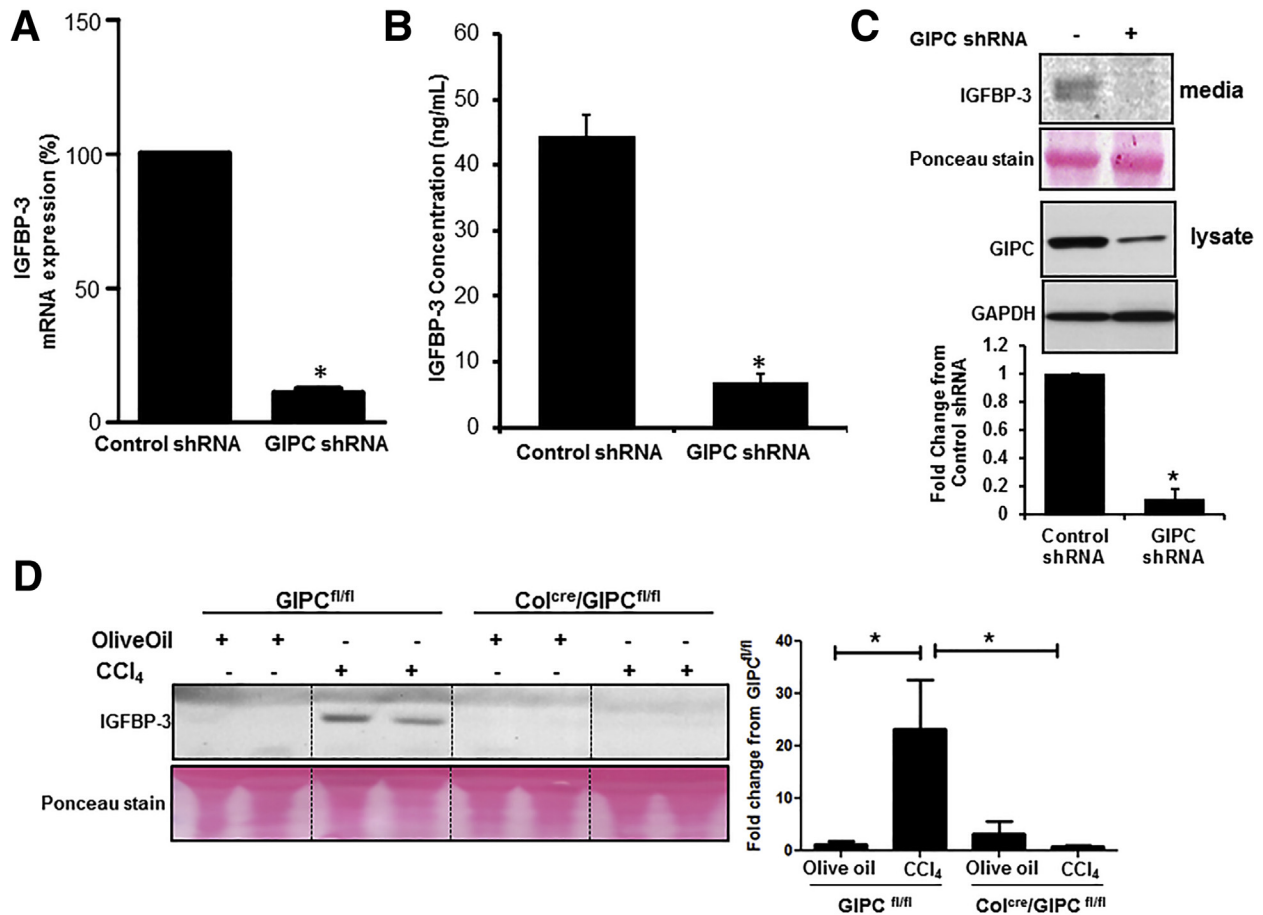


Figure 4. IGFBP-3 transcription and expression is regulated by GIPC. (A) GIPC was knocked down in human HSCs and cells were harvested for mRNA analysis. GIPC knockdown human HSCs showed a reduction in the mRNA levels of IGFBP-3. (B) Conditioned media was collected from serum-starved human HSCs with and without GIPC knockdown and was analyzed for IGFBP-3 secreted from the cells. Reduced IGFBP-3 production from human HSCs was observed on GIPC knockdown using ELISA and WB. (C) Immunoblot from cell lysates showed efficiency of GIPC knockdown, GAPDH was used as a loading control. (D) WB was performed from serum of GIPC^{fl/fl} and Col^{cre}/GIPC^{fl/fl} mice that received olive oil or CCl₄ injections intraperitoneally twice weekly for 4 weeks. IGFBP-3 was increased in serum from CCl₄-treated GIPC^{fl/fl} mice but not in Col^{cre}/GIPC^{fl/fl} mice. All data are shown as means \pm SEM. One-way analysis of variance with the Bonferroni multiple comparison tests were used to analyze groups for statistical significance. The Student unpaired *t* test was used to analyze the differences between 2 groups. **P* < .05. shRNA, short hairpin RNA.

alcoholic cirrhosis. IGFBP-3 serum levels were detected by WB and compared with healthy controls (*n* = 6). IGFBP-3 levels were increased significantly (Figure 7E). Taken together, these data indicate up-regulation of IGFBP-3 in cirrhosis, highlighting its possible role in human liver fibrogenesis including its potential use as a therapeutic target.

IGFBP-3 Promotes HSC Migration via β 1 Integrin Signaling and the Phosphatidylinositol 3-Kinase / Protein Kinase B Pathway, Which Requires Iron (Fe^{3+}) as Co-factor

Finally, we moved to in vitro studies to ascertain the mechanism of effect of IGFBP-3 on HSCs that could promote fibrosis in vivo. HSC migration is critical for HSC configuration and alignment around the sinusoids, which is required for sinusoidal contraction and perivascular matrix deposition. Therefore, we next examined the effect of IGFBP-3 on a

possible HSC migration–autocrine/paracrine amplification loop. We incubated HSCs with varying concentrations of IGFBP-3 (200 and 400 ng/mL), and measured HSC migration by wound assay. This showed a dose-dependent increase by IGFBP-3 on cell migration (Figure 8A). These data indicate a chemokinetic effect of IGFBP-3 on HSCs.

Integrins are transmembrane proteins involved in cell adhesion and migration by linking extracellular matrix proteins to the actin cytoskeleton. IGFBP-3 has been shown to form multimolecular complexes with integrin.^{25,26} By using a microfluidic flow chamber, we incubated HSCs with integrin β 1-neutralizing antibody and then treated cells with IGFBP-3 to study migration. IGFBP-3-mediated HSC migration was blocked with integrin β 1-neutralizing antibody (Figure 8B). We next examined the role of IGFBP-3 in cell proliferation. HSCs with IGFBP-3 knockdown showed a reduction in mRNA levels of Ki67, indicating the role of IGFBP-3 in cell proliferation as well (Figure 8C). IGFBP-3

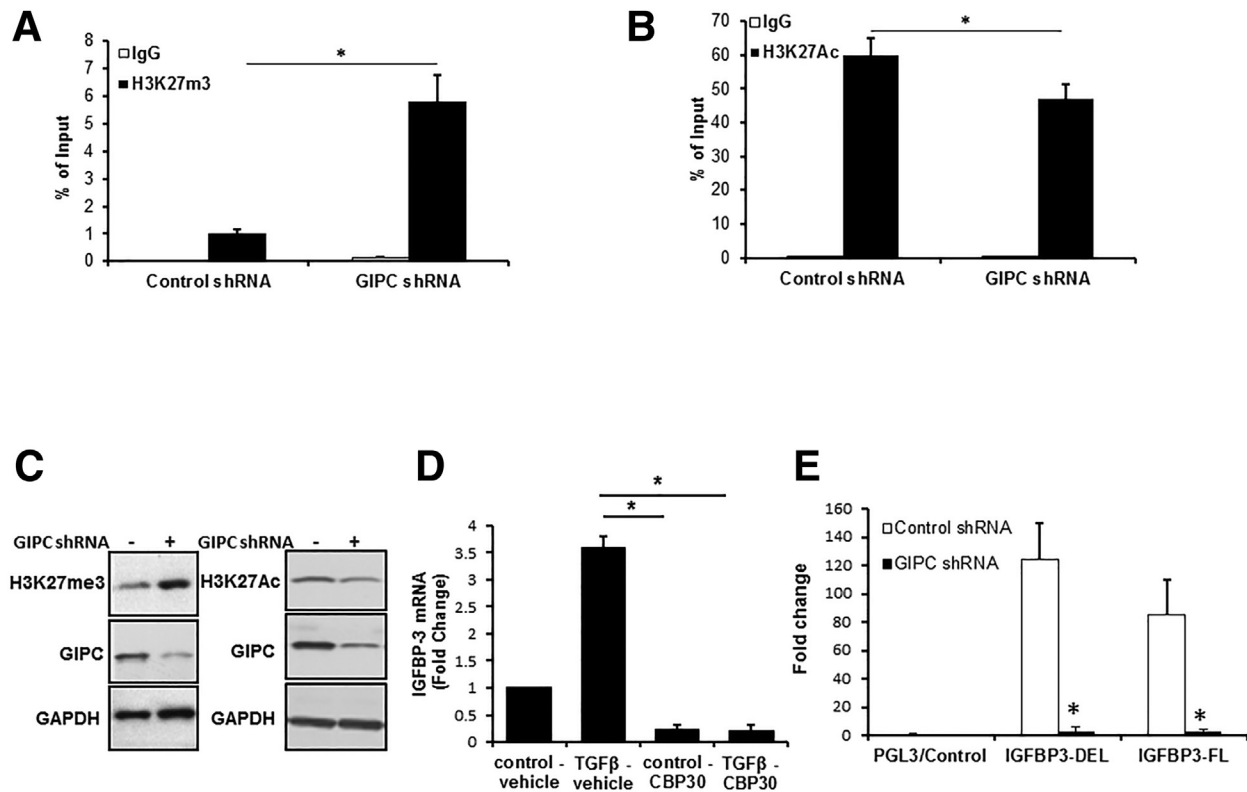


Figure 5. Knockdown of GIPC in human HSCs leads to decreased IGFBP-3 gene transcription via histone modifications. (A) ChIP using H3K27me3 antibody showed increased methylation of histone H3 at lysine 27 of the IGFBP-3 promoter after GIPC knockdown. (B) There was reduced acetylation of histone H3 at lysine 27 in GIPC knockdown human HSCs as shown by ChIP using the H3K27Ac antibody. (C) Lysates from human HSCs with GIPC knockdown showed increase levels of methylation of histone H3 at lysine 27 by WB. A reduction in acetylation of histone H3 at lysine 27 was observed in GIPC knockdown human HSCs compared with control cells. The efficiency of short hairpin RNA (shRNA)-mediated knockdown of GIPC also was shown with GAPDH as a loading control. (D) qPCR for IGFBP-3 from serum-starved human HSCs treated with cAMP-responsive element binding protein binding protein-30 (p300 inhibitor) showed a reduction in mRNA levels of IGFBP-3 after p300 inhibition. TGF- β treatment was used as a positive control. (E) IGFBP-3 promoter luciferase reporter plasmids were used in promoter analysis. Two sets of IGFBP-3 promoters were used; pGL3-IGFBP-3 full length (FL) (-3595 bp to +55 bp) and pGL3-IGFBP-3-deletion (Del) (-1950 bp to +55 bp). Constructs were transfected into human HSCs with and without GIPC knockdown, and luciferase activity was measured. GIPC silencing in human HSCs led to a significant reduction of activity of both promoter constructs. All data are shown as means \pm SEM. One-way analysis of variance with Bonferroni multiple comparison tests were used to analyze groups for statistical significance. * $P < .05$.

knockdown also was confirmed by qPCR (Figure 8D). From a signaling perspective, integrin $\beta 1$ can induce phosphorylation of AKT to promote cell migration. Therefore, we sought to test if IGFBP-3 may work through this signaling model to induce HSC chemokinesis and proliferation. Indeed, incubation of HSCs with increasing concentrations of IGFBP-3 (200 and 400 ng/mL) increased AKT phosphorylation as assessed by WB from HSC lysates (Figure 9A). Furthermore, AKT phosphorylation was attenuated by pre-incubation with integrin $\beta 1$ -neutralizing antibody 4 hours before IGFBP-3 treatment, although total AKT was not affected (Figure 9A). Finally, integrin and IGFBP-3 were proposed previously to form a multimolecular complex through Fe^{3+} .^{25,26} To show the involvement of Fe^{3+} in the IGFBP-3-induced AKT phosphorylation pathway, we treated HSCs with IGFBP-3 and different doses of Fe^{3+} . We found that Fe^{3+} enhanced IGFBP-3-induced AKT phosphorylation in a dose-dependent manner

(Figure 9B). Taken together, these results show that IGFBP-3 induces AKT activation through Fe^{3+} -enhanced integrin $\beta 1$ signaling to promote HSC migration.

Discussion

In this study, genome-wide expression profile experiments were conducted and followed by examination of chromatin dynamic events that regulate expression of IGFBP-3. The use of genetically modified mice, observations in patient-derived tissue, and, finally, in vitro signaling and functional studies allowed us to link these expression profile data with pathobiologically significant phenomena. The significant findings from these comprehensive analyses are as follows: (1) GIPC increases IGFBP-3 expression in HSCs through epigenetic modification on histone proteins; (2) IGFBP-3 knockdown attenuates liver fibrosis in vivo; (3) serum levels of IGFBP-3 are up-regulated in cirrhotic patients; and (4) IGFBP-3 promotes HSC activation and

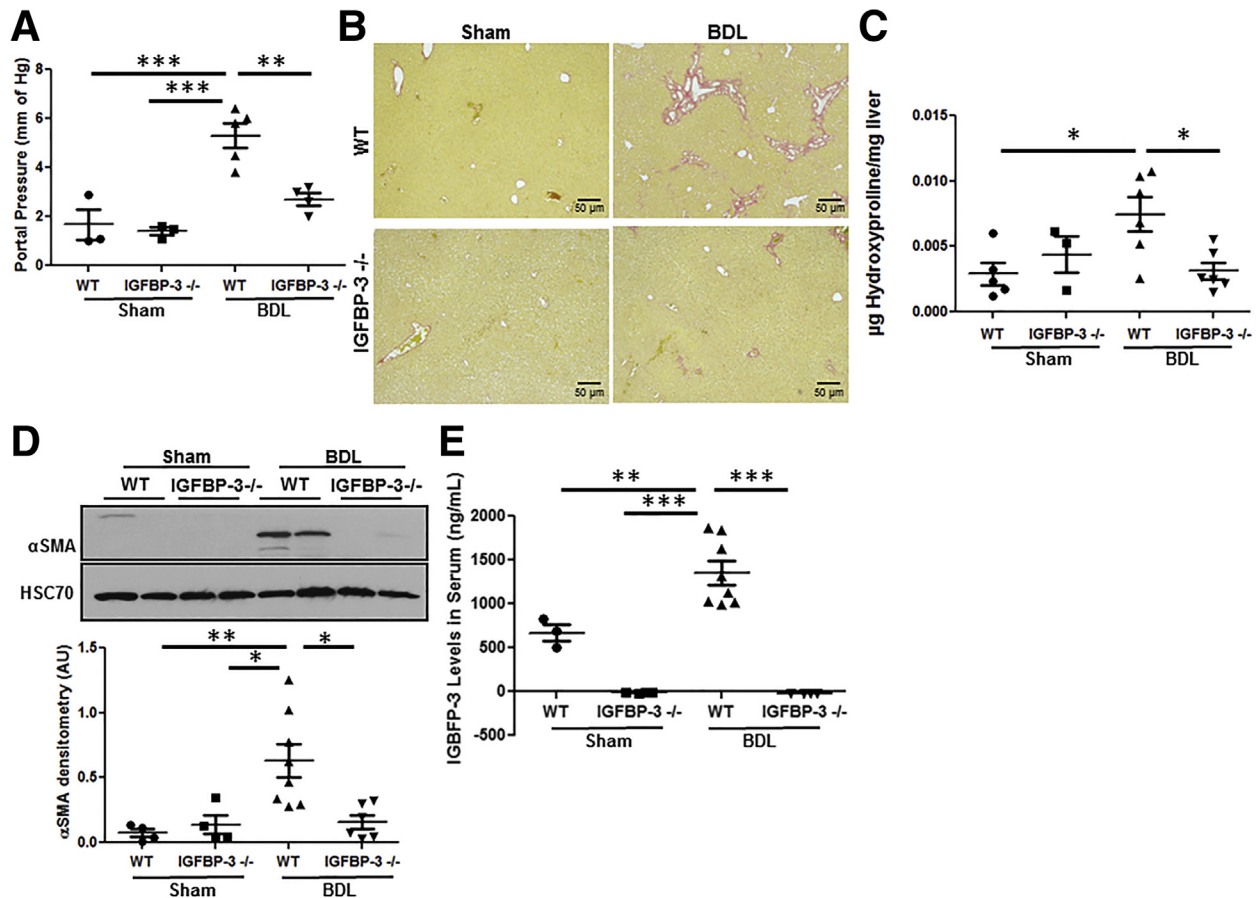


Figure 6. IGFBP-3^{-/-} mice are protected from BDL-induced fibrosis and portal hypertension. (A) Liver injury was induced in WT and IGFBP-3^{-/-} mice by BDL. IGFBP-3^{-/-} mice showed lower portal pressure after BDL surgery compared with WT mice. (B) Liver sections from IGFBP-3^{-/-} mice after BDL surgery show lower Sirius red staining compared with WT mice. (C) Collagen content was reduced in IGFBP-3^{-/-} mice compared with WT mice after BDL surgery as measured by a hepatic hydroxyproline assay. (D) α SMA levels were lower in IGFBP-3^{-/-} mice compared with WT mice after BDL surgery by WB. (E) Serum levels of IGFBP-3 were quantified by ELISA from WT and IGFBP-3^{-/-} mice after sham and BDL. IGFBP-3 levels in serum were increased in BDL compared with sham mice, whereas IGFBP-3^{-/-} mice had no IGFBP-3 detected. All data are shown as means \pm SEM. Each dot in the scatter plot indicates an individual animal in each of the panels. One-way analysis of variance with Bonferroni multiple comparison tests were used to analyze groups for statistical significance. * $P < .05$, ** $P < .001$, *** $P < .0001$.

migration through integrin-AKT signaling. [Figure 10](#) summarizes these key findings, which are discussed in the following sections in more detail.

TGF- β activation of HSCs contributes to liver fibrosis.²⁷ In this study we compared expression profiles of normal HSCs, with profiles of HSCs treated with TGF- β by mRNA sequencing. We identified IGFBP-3 as one of the top TGF- β -induced targets alongside canonical genes such as collagen and fibronectin. Given our recent insights into the role of the scaffold protein GIPC in receptor signaling and HSC activation,⁷ we performed another mRNA sequencing analysis of TGF- β -stimulated HSCs with GIPC knockdown. GIPC has been shown to link receptor activation with intracellular signaling and gene transcription.⁷ We previously showed that GIPC regulates receptor protein stability, function, and, ultimately, cell migration in HSCs.⁷ We now link GIPC mechanisms of action through its downstream transcriptional target IGFBP-3.

IGFBP-3 originally was identified as an IGF transport protein with multifunctional properties achieved in part by blocking the interaction between IGF 1/2 and its IGF receptor.⁹ Our in vitro data comparing different types of liver cell lines and our single-cell RNA sequencing data ([Figure 3](#)) are consistent with a recent single-cell RNA sequencing study,²⁸ indicating that HSCs are the major liver cell type to produce IGFBP-3 in control mice (received olive oil) and in response to chronic CCl₄ in mice. More importantly, 2 recent single cell RNA sequencing studies of human liver also showed that HSCs and mesenchymal cells are the major liver cell types that produce IGFBP-3.^{29,30} Indeed, IGFBP-3 has been shown previously to activate HSCs based on gene expression profiling studies from quiescent and activated HSCs.¹⁶ The present study identifies mechanisms by which this occurs.

We show that IGFBP-3 expression and release from HSC is decreased on GIPC knockdown in vitro and in vivo. Our data indicate that GIPC can increase IGFBP-3 transcription

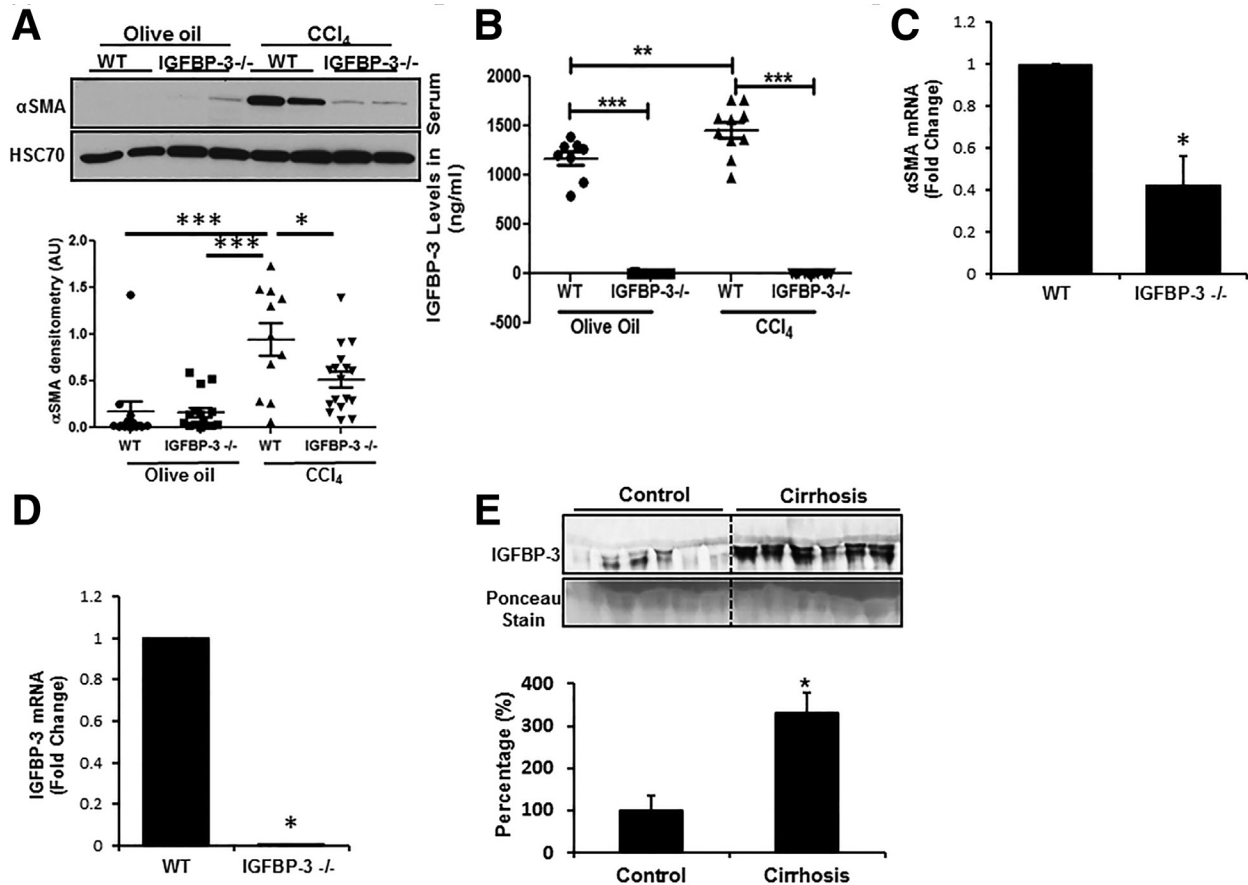


Figure 7. IGFBP-3^{-/-} mice show attenuated HSC activation in response to chronic CCl₄. (A) IGFBP-3^{-/-} or genotype control mice were injected with olive oil or CCl₄ intraperitoneally to induce liver fibrosis. α SMA levels were lower in IGFBP-3^{-/-} mice after chronic CCl₄ administration compared with control mice by WB of whole-liver lysates. Densitometric analysis also is shown. (B) ELISA shows an increase in serum levels of IGFBP-3 in CCl₄-administered mice and loss of IGFBP-3 protein in serum from IGFBP-3^{-/-} mice. (C) HSCs isolated from IGFBP-3^{-/-} and WT mice were used to detect the mRNA level of α SMA by qPCR. (D) IGFBP-3 knockout was confirmed by qPCR. (E) WB from serum of patients with cirrhosis showed increased levels of IGFBP-3 compared with controls. All data are shown as means \pm SEM. Each dot in the scatter plot indicates an individual animal in each of the panels. One-way analysis of variance with Bonferroni multiple comparison tests were used to analyze groups for statistical significance. * $P < .05$, ** $P < .001$, *** $P < .0001$.

through epigenetic changes characterized by a decrease in H3K27 trimethylation, and a reciprocal increase in H3K27 acetylation. The GIPC-induced increase in IGFBP-3 is mediated through the acetyltransferase p300, which is responsible for the acetylation of H3K27 within the promoter region of IGFBP-3. The observed histone methylation (H3K27m3) is regulated by EZH2, a methyltransferase.²⁷ EZH2 is the functional enzymatic component of the polycomb repressive complex 2, which is responsible for the methylation activity of the polycomb repressive complex 2 on histone 3 lysine 27 (H3k27), together with other proteins required for optimal repression such as SUZ12.^{27,31} Comparison of the luciferase activity of the truncation construct of IGFBP-3 promoter and the full length suggests that +55 bp to -1950 bp of the IGFBP-3 transcription start site indeed contains the EZH2 binding motif and may be required for H3K27m3 repression induced by GIPC knockdown. Previous studies have implicated DNA acetylation as a regulatory mechanism of IGFBP-3 as well,^{20,21} which may complement

our observations related to histone acetylation. GIPC regulates PDGFR β expression in HSCs in a similar way to what we observed with IGFBP-3.⁷ Indeed, knockdown of GIPC decreases H3K27Ac and increases H3K27me3 levels to regulate PDGFR β .⁷ We conclude that expression of IGFBP-3 is tightly controlled by these epigenetic modifications and these 2 key enzymes. Both enzymes therefore might be used as upstream targets to regulate IGFBP-3 as well as PDGFR β , potentially to provide a greater therapeutic benefit.⁷

Our in vivo studies have shown that global deletion of IGFBP-3 significantly reduces liver fibrosis and portal hypertension in response to chronic liver injury. Mechanistically, this raises an important question: does IGFBP-3 regulate portal hypertension only through effects on fibrosis or also through effects on vascular resistance, and, if the latter, are effects only on HSCs or also on liver sinusoidal endothelial cells (LSEC)? We did not observe an effect of IGFBP-3 on collagen mRNA levels in vitro (control siRNA 1.02 \pm 0.03 vs IGFBP-3 siRNA 0.98 \pm 0.02 [fold change] by qPCR), but we did see reduced matrix

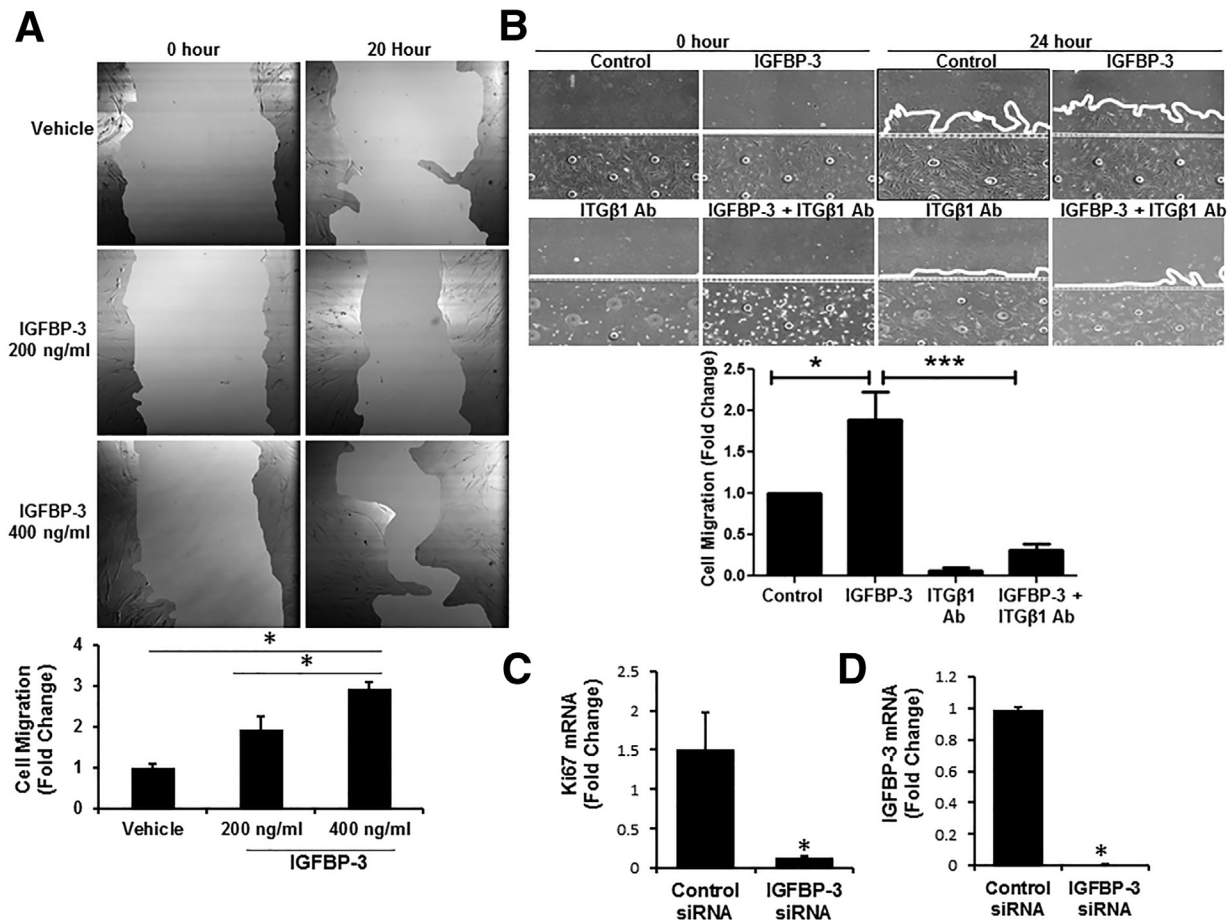


Figure 8. IGFBP-3 promotes cell migration in human HSCs in an integrin $\beta 1$ -dependent manner. (A) Confluent monolayer of human HSCs serum-starved overnight was scratched and incubated with recombinant IGFBP-3 in a dose mentioned with the corresponding figure and images were captured. IGFBP-3 promoted cell migration in human HSCs in a concentration-dependent fashion as shown by wounding assay. Representative images are shown in the panel with quantification represented by a graph. (B) Recombinant human IGFBP-3 was incubated with human HSCs in a microfluidic chamber system and migration was assessed. Human HSCs were incubated with integrin $\beta 1$ -neutralizing antibody with and without IGFBP-3, and migration was quantified. In the presence of integrin $\beta 1$ -neutralizing antibody, migration was reduced in response to IGFBP-3. Quantification of migration is shown in the graph with representative images. (C) qPCR from human HSCs with and without IGFBP-3 knockdown showed a reduction in Ki67 mRNA, which is a marker for cell proliferation. (D) The efficiency of IGFBP-3 knockdown is shown. One-way analysis of variance with Bonferroni multiple comparison tests used to analyze groups for statistical significance. The Student unpaired *t* test was used to analyze the differences between 2 groups. **P* < .05. Ab, antibody.

deposition in IGFBP-3^{-/-} mice exposed to chronic liver injury. Given that IGFBP-3 increased HSC migration and proliferation in vitro, we hypothesize that the effect of IGFBP-3 on fibrosis in vivo is the result of HSC mass and migration rather than transcriptional activation of collagen in HSCs. Therefore, in vivo it is likely that both increased fibrosis and increased HSC contraction of sinusoids contributes to IGFBP-3 driving portal hypertension.³² To examine for potential effects of IGFBP-3 on LSECs, murine LSECs were treated with recombinant IGFBP-3, and tube angiogenesis, a canonical function of endothelial cells, which is thought to contribute to portal hypertension,³³ was examined. There was no difference in cells treated with IGFBP-3 compared with control (control 1.0 ± 0.2 vs IGFBP-3 0.95 ± 0.1 [fold change]). Based on these results, we propose that IGFBP-3 does not influence LSEC defects, which characterize portal hypertension, but rather its effects are on HSCs directly.

Although our proposed role of IGFBP-3 is consistent with a prior correlative study implicating IGFBP-3 with HSC activation,¹⁶ it is in contradistinction to a recent study that showed that IGFBP-3 has anti-inflammatory effects in hepatocytes.³⁴ IGFBP-3 also has been implicated in tumor-suppressive properties in non-small-cell lung cancer, glioblastoma, and, more recently, neuroblastoma.³⁵⁻³⁷ These divergent effects of IGFBP-3 likely are dependent on the cell type that is both producing and responding to the molecule. For example, tumor-suppressive actions of IGFBP-3 may occur through ligand binding with IGF and IGFR.³⁸ In hepatocytes, IGFBP-3 is thought to inhibit nuclear factor- κ B and proinflammatory cytokines via IGFBP-3-receptor-mediated activation of caspases.³⁴ Eventually, cell-selective rather than global knockout of IGFBP-3 will be useful to clarify cell-specific actions of IGFBP-3.

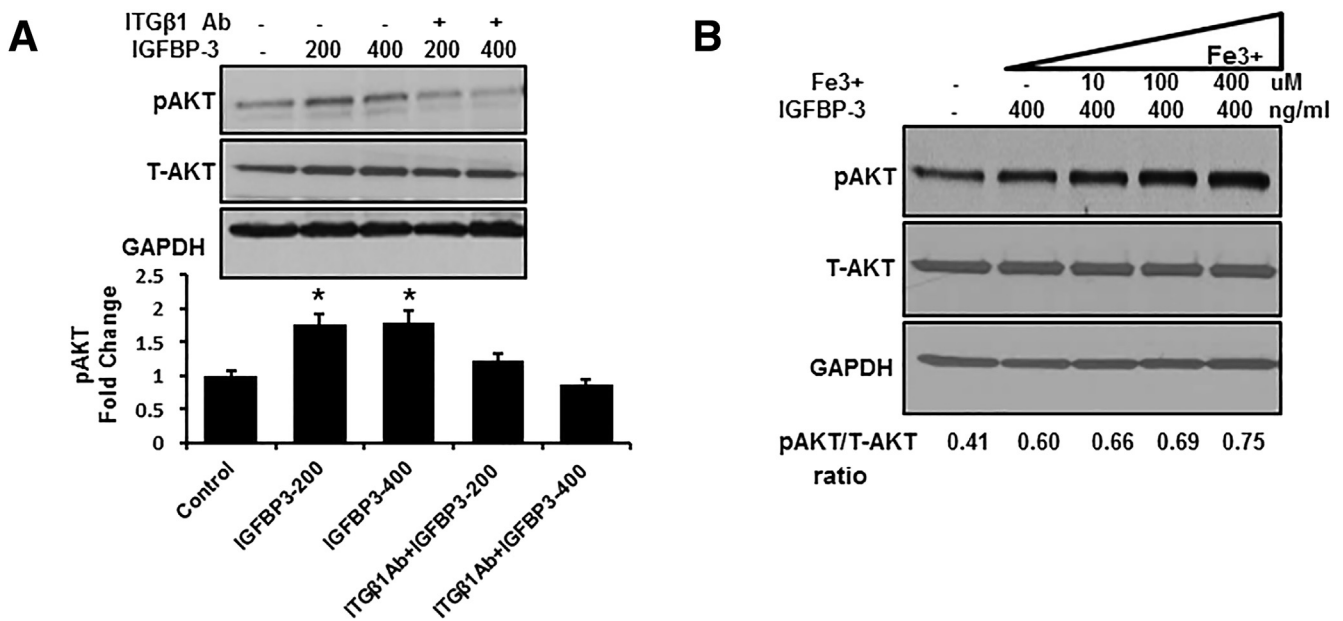


Figure 9. IGFBP-3 induces activation of AKT through integrin $\beta 1$. (A) Serum-starved human HSCs were treated with IGFBP-3 and integrin $\beta 1$ -neutralizing antibody and lysates were collected and analyzed for WB. Immunoblots evidenced activation of AKT by IGFBP-3, which was blocked by integrin $\beta 1$ -neutralizing antibody. Total AKT and GAPDH were used as a loading control. (B) WB from lysates of serum-starved human HSCs were treated with recombinant IGFBP-3 with and without Fe^{3+} in a dose-response fashion as indicated. The entire concentration response curve was performed in duplicate. IGFBP-3-mediated activation of AKT in human HSCs was enhanced with the addition of Fe. Total AKT and GAPDH were used as a loading control. Densitometric analysis of immunoblots is shown under the blot. All data are shown as means \pm SEM. One-way analysis of variance with Bonferroni multiple comparison tests were used to analyze groups for statistical significance. * $P < .05$, *** $P < .0001$. Ab, Antibody; pAkt, phospho protein kinase B; T-AKT, total protein kinase B.

IGFBP-3 has been shown as a marker of HSC activation and implicated in cell migration in a variety of cell types.^{39–41} However, the mechanism by which this occurs is not clear. Our wounding assay and microfluidic models confirmed that IGFBP-3 promotes HSC migration. Signaling studies have shown that this occurs through an integrin $\beta 1$ -AKT-dependent pathway. Insulin-like growth factor-I-independent functions of IGFBP-3 may be achieved through binding with metals such as iron,⁴¹ this results in conformational changes that expose the metal binding domain epitope to enhance interaction with cell surface targets such as integrins.⁴¹ It is known that chronic liver diseases such as viral hepatitis, alcoholic liver disease, and nonalcoholic fatty liver disease are associated with increased hepatocellular, sinusoidal, or mixed-pattern iron loading.^{42,43} The increased free iron seems to be associated with disease progression because it poses a highly reactive form, and pro-oxidant forms of iron eventually are diverted toward liver parenchymal cells, where they may fuel oxidative damage.⁴⁴ Indeed, we found that Fe^{3+} enhances IGFBP-3-induced AKT phosphorylation in an integrin- and dose-dependent manner. Our finding extends the role of iron in IGFBP-3 function, which is independent from IGF. It is interesting to speculate that iron/IGFBP-3 interactions could contribute to the potential hepatotoxicity of iron in vivo.⁴⁵

In the present study, we show that IGFBP-3 promotes HSC migration by iron-enabled binding to integrin $\beta 1$ -mediating AKT signaling. Global deletion of IGFBP-3 also attenuates liver fibrosis and portal hypertension in vivo.

These findings provide evidence that the aforementioned increased serum IGFBP-3 levels and increased IGFBP-3 expression in the mesenchymal cell cluster of single-cell RNA sequencing, detected in cirrhotic patients,³⁰ may indeed be of functional relevance and make IGFBP-3 an interesting biomarker⁴⁶ or target for antifibrotic treatment.

Methods

Cell Lines and Transfection

Human primary HSCs (catalogue 5300; ScienCell Research Laboratories, Carlsbad, CA) were cultured in Dulbecco's modified Eagle medium supplemented with 10% fetal bovine serum and penicillin/streptomycin. Experiments were performed after overnight serum starvation. Small interfering RNA (siRNA) for IGF1R, integrin $\beta 1$, and IGFBP-3 were purchased from Qiagen (Venlo, The Netherlands). GIPC short hairpin RNAs were a gift from Dr Mukhopadhyay (Mayo Clinic, Rochester, MN) and purchased from Sigma-Aldrich (NM_005716.2-1083s1c1, NM_005716.2-1045s1c1; St. Louis, MO). Lentiviral transduction of short hairpin RNA was performed by incubation with viral particles for 48 hours in Dulbecco's modified Eagle medium with 10% fetal bovine serum and polybrene, followed by selection with puromycin for 24 hours.

Compounds and Ligands

IGFBP-3 and IGF1 were purchased from Sigma-Aldrich and used at concentrations of 200 and 400 ng/mL, respectively, in

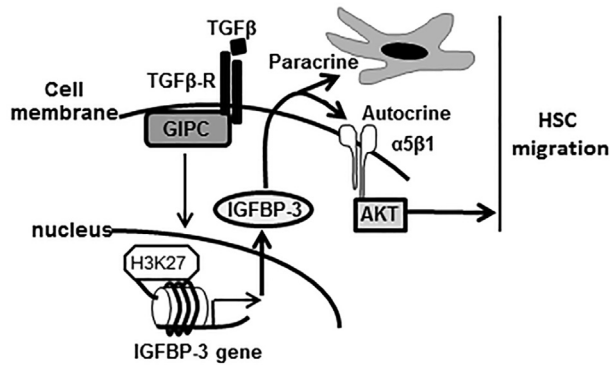


Figure 10. The proposed mechanism of IGFBP-3 in the regulation of HSC migration. IGFBP-3 expression is up-regulated by GIPC through epigenetic changes characterized by a decrease of H3K27 trimethylation and a reciprocal increase in H3K27 acetylation after activation of the TGF receptor. Furthermore, IGFBP-3 promotes HSC migration by iron-enabled binding to integrin $\beta 1$ and mediates AKT signaling, leading to autocrine and paracrine HSC migration. Akt, protein kinase B.

basal media overnight unless otherwise stated in the Figure legends 8 and 9. AKT inhibitor and cAMP-responsive element binding protein binding protein30 (p300 inhibitor) were used at a dilution of 1:1000. PDGF-BB (R&D Systems, Minneapolis, MN) was used at a concentration of 10 ng/mL.

Antibodies

Primary antibodies were used at a concentration of 1:1000 (except for glyceraldehyde-3-phosphate dehydrogenase [GAPDH], for which the dilution was 1:5000) in 5% dry milk/Tris-buffered saline/1% Tween 20 with overnight incubation at 4°C. Secondary antibodies (donkey anti-rabbit + horseradish peroxidase or sheep anti-mouse + horseradish peroxidase) were used at a concentration of 1:1000 (except for GAPDH, for which the secondary antibody was used at a dilution of 1:3000) for 1 hour at room temperature in Tris-buffered saline/1% Tween 20. Membranes were developed with luminol solution. Primary antibodies for IGFBP-3, IGFR, phosphorylated IGFR, phosphorylated AKT, phosphorylated extracellular signal-regulated kinase, H3K27Ac, and H3K27m3 all were purchased from Cell Signaling Technology (Danvers, MA). GAPDH was purchased from Sigma Aldrich, and GIPC antibody was purchased from Proteus Bioscience (Ramona, CA).

RNA Isolation, Complementary DNA Synthesis, and Quantitative Real-Time PCR

Total RNA was extracted from HSCs according to the manufacturer's instructions using an RNeasy kit (Qiagen), and 5 μ g RNA was used for complementary DNA synthesis with oligo (deoxythymine) primer using the SuperScript III first-strand synthesis system for reverse-transcription PCR (Invitrogen, Carlsbad, CA) per the manufacturer's protocol. Real-time PCR was performed in a total 25- μ L volume reaction using Sybr Green Master Mix and the 7500 real-time PCR

system (both from Applied Biosystems, NY), according to the manufacturer's instructions. Reverse-transcription PCR analysis was performed with the following primer sets: human GIPC forward: 5'-GCTGGAGAGTTACATGGGTATC-3'; human GIPC reverse: 5'-TCAGGGAAGGCAAAGTCAC-3'; mouse GIPC forward: 5'-GAAGGTGGATGACTTGCTAGAG-3'; and mouse GIPC reverse: 5'-TCATCTGGGAATGCGAAGTC-3'; and human IGFBP-3 forward: 5'-GCGGCCGCATGGG-GACTTCCCATCC-3'; human IGFBP-3 reverse: 5'-CTCGAG-CAGGAAGCTGTCTTCCACC-3'. Amplification of human GAPDH and mouse β -actin was performed in the same reaction for respective samples as internal controls. Each experiment was performed in triplicate.

RNA Sequencing and Analysis

mRNA sequencing libraries were prepared and sequenced on an Illumina (Mayo Clinic, Rochester, MN) HiSeq 2000 instrument at the Mayo Clinic Center for Individualized Medicine Medical Genomics Facility. Sequence reads from RNA sequencing samples were aligned to the human genome hg19 and gene annotations from Refseq gene using TopHat v2.0.5. Cufflinks v2.0.2 was used to calculate FPKM values of genes. Differential gene expression was analyzed by Cuffdiff using a cut-off false-discovery rate of less than 0.05, and an absolute value of $\log_{2}FC \geq 2$. Single-cell RNA sequencing has been done with liver cells including hepatic stellate cells from control and CCl4 mice for barcoding and sequencing in NGS core at Mayo Clinic Rochester MN as per 10X Genomics protocol (<https://www.10xgenomics.com/single-cell-technology/>). The hepatic stellate cells clusters were analyzed by Loupe cell browser in this article.

ChIP Analysis

ChIP was performed with EZ-Magna ChIP (catalog #17-408; Millipore, Burlington, MA) with specific immunoprecipitating antibodies including H3K27Me3 or H3K27Ac, with the negative control normal rabbit IgG as previously described.⁷ Cells were cross-linked with 1% formaldehyde, after which they were lysed and subjected to sonication, then sheared cross-linked to fragment DNA. After centrifugation, the supernatant was diluted in ChIP buffer. Samples subsequently were incubated with 5 μ g antibody and ChIP-grade Protein A magnetic beads (Millipore) overnight at 4°C. After extensive washing (Low Salt, High Salt, LiCl Immune Complex Wash Buffer, and TE Buffer; Sigma-Aldrich Inc, St. Louis, MO), chromatin was eluted, and DNA was purified and analyzed by qPCR. Fold enrichment was calculated by first normalizing ChIP-qPCR to input DNA of the target gene as a percentage of input. This subsequently was normalized to the percentage input of a negative control gene region (intergenic region of 36Me3-hCh19) to correct for experimental variation. H3K27Ac (4279), H3K27me3 (6002), and isotype-specific IgG control (2027) were purchased from Abcam (Cambridge, MA).

Cell Migration Functional Assays

HSCs were grown to a confluent monolayer in a 6-well tissue culture plate before scratch being induced with a

10- μ L pipette tip. Media was changed with an appropriate stimulant at the time of scratch. Cells were imaged at 0 and 6 hours after scratch. The total area of the scratch was measured using ImageJ software (National Institutes of Health, Bethesda, MD), and the percentage of migration area was calculated by the following formula: (area time 0 h - area time 6 h)/area time 0 h.

Microfluidic Cell Migration Imaging

A 2-cell-chamber microfluidic device was used for the cell migration experiment. Presterilized microfluidic platforms were coated initially with collagen solution (0.2 mg/mL). Both cell chambers were kept separated by sealing the microgrooves. A total of 15–20 μ L of the cell suspension at a density of approximately 5000 cells/ μ L media was added to 1 chamber with pillars. The other chamber was used to add recombinant IGFBP-3 into media. HSCs were treated with vehicle or integrin β 1-neutralizing antibody. Chambers were imaged and analyzed for cell migration as previously described.⁷

Animal Studies

All animal experiments were approved by the Institutional Animal Care and Use Committee and performed in accordance with institutional guidelines. Embryos from IGFBP-3^{-/-} (insulin-like growth factor binding protein 3; targeted mutation 1, Velocigene (Igfbp3tm1(KOMP)Vlcg) were purchased from the UC-Davis (Davis, CA) mouse repository. The embryos were injected in a foster mother and subsequent progeny were mated for germline production and colony expansion. IGFBP-3^{-/-} mice (age, 8–10 wk) and background control strain mice (age matched) (C57BL/6NTac) with an initial body weight of approximately 25 g were used. GIPC^{fl/fl} mice were crossed with collagen^{cre} mice to generate GIPC^{fl/fl}/collagen^{cre} mice that were genetically depleted of GIPC in myofibroblasts. Cre-negative littermate controls were used for in vivo experiments. Mice underwent a twice-weekly intraperitoneal injection of 0.5 mg/kg body weight of CCl₄ for 6 weeks. Serum and livers were harvested at week 6 for WB, hydroxyproline assay, ELISA, and immunofluorescence as described previously.^{3,47} Eight-week-old WT and IGFBP-3^{-/-} mice were divided into 2 groups. One group underwent BDL surgery as described previously,⁴⁷ and the other group received sham surgery. After 4 weeks, portal pressure was measured before killing the mice as described previously.⁴⁸ Serum and livers were collected for hydroxyproline, WB, ELISA, and immunofluorescence. IGFBP-3 levels were measured in serum by the mouse IGFBP-3 Quantikine ELISA kit (R&D Systems, Inc) according to the manufacturer's instructions, and by a SpectraMax Plus 384 microplate reader (Molecular Devices, San Jose, CA).

Clinical Samples

Serum of control and alcoholic cirrhotic patients were collected and analyzed by WB to detect IGFBP-3 proteins. Clinical and demographic information about this cohort was published recently.⁷ Patient studies were approved by the Institutional Review Board at the Mayo Clinic (Rochester, MN).

Statistics

Experiments were performed at least 3 independent times and numeric data are expressed as means \pm SEM. The significance of the differences of the means was evaluated by a paired and unpaired 2-tailed Student *t* test. A *P* value less than .05 was considered significant.

Study Approval

All animal experiments were approved by the IACUC and performed in accordance with institutional guidelines (Mayo Clinic). Patient sample use was approved by the Institutional Review Board at the Mayo Clinic.

References

- Henderson NC, Iredale JP. Standing down the guard: stellate cells leave quietly. *Gastroenterology* 2012; 143:890–892.
- Mogler C, Wieland M, Konig C, Hu J, Runge A, Korn C, Besemfelder E, Breitkopf-Heinlein K, Komljenovic D, Dooley S, Schirmacher P, Longerich T, Augustin HG. Hepatic stellate cell-expressed endosialin balances fibrogenesis and hepatocyte proliferation during liver damage. *EMBO Mol Med* 2015;7:332–338.
- Cao S, Yaqoob U, Das A, Shergill U, Jagavelu K, Huebert RC, Routray C, Abdelmoneim S, Vasdev M, Leof E, Charlton M, Watts RJ, Mukhopadhyay D, Shah VH. Neuropilin-1 promotes cirrhosis of the rodent and human liver by enhancing PDGF/TGF-beta signaling in hepatic stellate cells. *J Clin Invest* 2010; 120:2379–2394.
- Granzow M, Schierwagen R, Klein S, Kowallick B, Huss S, Linhart M, Mazar IG, Gortzen J, Vogt A, Schildberg FA, Gonzalez-Carmona MA, Wojtalla A, Kramer B, Nattermann J, Siegmund SV, Werner N, Furst DO, Laleman W, Knolle P, Shah VH, Sauerbruch T, Trebicka J. Angiotensin-II type 1 receptor-mediated Janus kinase 2 activation induces liver fibrosis. *Hepatology* 2014;60:334–348.
- Yaqoob U, Cao S, Shergill U, Jagavelu K, Geng Z, Yin M, de Assuncao TM, Cao Y, Szabolcs A, Thorgeirsson S, Schwartz M, Yang JD, Ehman R, Roberts L, Mukhopadhyay D, Shah VH. Neuropilin-1 stimulates tumor growth by increasing fibronectin fibril assembly in the tumor microenvironment. *Cancer Res* 2012; 72:4047–4059.
- Iwakiri Y. Pathophysiology of portal hypertension. *Clin Liver Dis* 2014;18:281–291.
- Drinane MC, Yaqoob U, Yu H, Luo F, Greuter T, Arab JP, Kostallari E, Verma VK, Maiers J, De Assuncao TM, Simons M, Mukhopadhyay D, Kisseleva T, Brenner DA, Urrutia R, Lombark G, Gao Y, Ligresti G, Tschumperlin DJ, Revzin A, Cao S, Shah VH. Synectin promotes fibrogenesis by regulating PDGFR isoforms through distinct mechanisms. *JCI Insight* 2017;2.
- Masters TA, Tumbarello DA, Chibalina MV, Buss F. MYO6 regulates spatial organization of signaling endosomes driving AKT activation and actin dynamics. *Cell Rep* 2017;19:2088–2101.

9. Baxter RC. IGF binding proteins in cancer: mechanistic and clinical insights. *Nat Rev Cancer* 2014;14:329–341.
10. Wang YA, Sun Y, Palmer J, Solomides C, Huang LC, Shyr Y, Dicker AP, Lu B. IGFBP3 modulates lung tumorigenesis and cell growth through IGF1 signaling. *Mol Cancer Res* 2017;15:896–904.
11. Ichikawa T, Nakao K, Hamasaki K, Furukawa R, Tsuruta S, Ueda Y, Taura N, Shibata H, Fujimoto M, Toriyama K, Eguchi K. Role of growth hormone, insulin-like growth factor 1 and insulin-like growth factor-binding protein 3 in development of non-alcoholic fatty liver disease. *Hepatol Int* 2007;1:287–294.
12. Pilewski JM, Liu L, Henry AC, Knauer AV, Feghali-Bostwick CA. Insulin-like growth factor binding proteins 3 and 5 are overexpressed in idiopathic pulmonary fibrosis and contribute to extracellular matrix deposition. *Am J Pathol* 2005;166:399–407.
13. Ruiz XD, Mlakar LR, Yamaguchi Y, Su Y, Larregina AT, Pilewski JM, Feghali-Bostwick CA. Syndecan-2 is a novel target of insulin-like growth factor binding protein-3 and is over-expressed in fibrosis. *PLoS One* 2012;7:e43049.
14. Baxter RC. Nuclear actions of insulin-like growth factor binding protein-3. *Gene* 2015;569:7–13.
15. Ricort JM, Binoux M. Insulin-like growth factor (IGF) binding protein-3 inhibits type 1 IGF receptor activation independently of its IGF binding affinity. *Endocrinology* 2001;142:108–113.
16. Mannaerts I, Schroyen B, Verhulst S, Van Lommel L, Schuit F, Nyssen M, van Grunsven LA. Gene expression profiling of early hepatic stellate cell activation reveals a role for Igfbp3 in cell migration. *PLoS One* 2013;8:e84071.
17. Zhou VW, Goren A, Bernstein BE. Charting histone modifications and the functional organization of mammalian genomes. *Nat Rev Genet* 2011;12:7–18.
18. Lin WH, Martin JL, Marsh DJ, Jack MM, Baxter RC. Involvement of insulin-like growth factor-binding protein-3 in the effects of histone deacetylase inhibitor MS-275 in hepatoma cells. *J Biol Chem* 2011;286:29540–29547.
19. Regel I, Eichenmuller M, Joppien S, Liebl J, Haberle B, Muller-Hocker J, Vollmar A, von Schweinitz D, Kappler R. IGFBP3 impedes aggressive growth of pediatric liver cancer and is epigenetically silenced in vascular invasive and metastatic tumors. *Mol Cancer* 2012;11:9.
20. Perks CM, Holly JM. Epigenetic regulation of insulin-like growth factor binding protein-3 (IGFBP-3) in cancer. *J Cell Commun Signal* 2015;9:159–166.
21. Walker GE, Wilson EM, Powell D, Oh Y. Butyrate, a histone deacetylase inhibitor, activates the human IGF binding protein-3 promoter in breast cancer cells: molecular mechanism involves an Sp1/Sp3 multiprotein complex. *Endocrinology* 2001;142:3817–3827.
22. Ebrahimi A, Sevinc K, Gurhan Sevinc G, Cribbs AP, Philpott M, Uyulur F, Morova T, Dunford JE, Goklemes S, Ari S, Oppermann U, Onder TT. Bromodomain inhibition of the coactivators CBP/EP300 facilitate cellular reprogramming. *Nat Chem Biol* 2019;15:519–528.
23. Cabbage ML, Suwanichkul A, Powell DR. Insulin-like growth factor binding protein-3. Organization of the human chromosomal gene and demonstration of promoter activity. *J Biol Chem* 1990;265:12642–12649.
24. Peng L, Malloy PJ, Feldman D. Identification of a functional vitamin D response element in the human insulin-like growth factor binding protein-3 promoter. *Mol Endocrinol* 2004;18:1109–1119.
25. Singh B, Charkowicz D, Mascarenhas D. Insulin-like growth factor-independent effects mediated by a C-terminal metal-binding domain of insulin-like growth factor binding protein-3. *J Biol Chem* 2004;279:477–487.
26. Yen YC, Hsiao JR, Jiang SS, Chang JS, Wang SH, Shen YY, Chen CH, Chang IS, Chang JY, Chen YW. Insulin-like growth factor-independent insulin-like growth factor binding protein 3 promotes cell migration and lymph node metastasis of oral squamous cell carcinoma cells by requirement of integrin beta1. *Oncotarget* 2015; 6:41837–41855.
27. Martin-Mateos R, De Assuncao TM, Arab JP, Jalan-Sakrikar N, Yaqoob U, Greuter T, Verma VK, Mathison AJ, Cao S, Lomberk G, Mathurin P, Urrutia R, Huebert RC, Shah VH. Enhancer of zeste homologue 2 inhibition attenuates TGF-beta dependent hepatic stellate cell activation and liver fibrosis. *Cell Mol Gastroenterol Hepatol* 2019;7:197–209.
28. Dobie R, Wilson-Kanamori JR, Henderson BEP, Smith JR, Matchett KP, Portman JR, Wallenborg K, Picelli S, Zagorska A, Pendem SV, Hudson TE, Wu MM, Budas GR, Breckenridge DG, Harrison EM, Mole DJ, Wigmore SJ, Ramachandran P, Ponting CP, Teichmann SA, Marioni JC, Henderson NC. Single-cell transcriptomics uncovers zonation of function in the mesenchyme during liver fibrosis. *Cell Rep* 2019; 29:1832–1847 e8.
29. MacParland SA, Liu JC, Ma XZ, Innes BT, Bartczak AM, Gage BK, Manuel J, Khuu N, Echeverri J, Linares I, Gupta R, Cheng ML, Liu LY, Camat D, Chung SW, Seliga RK, Shao Z, Lee E, Ogawa S, Ogawa M, Wilson MD, Fish, Selzner M, Ghanekar A, Grant D, Greig P, Sapisochin G, Selzner N, Winegarten N, Adeyi O, Keller G, Bader GD, McGilvray ID. Single cell RNA sequencing of human liver reveals distinct intrahepatic macrophage populations. *Nat Commun* 2018;9:4383.
30. Ramachandran P, Dobie R, Wilson-Kanamori JR, Dora EF, Henderson BEP, Luu NT, Portman JR, Matchett KP, Brice M, Marwick JA, Taylor RS, Efremova M, Vento-Tormo R, Carragher NO, Kendall TJ, Fallowfield JA, Harrison EM, Mole DJ, Wigmore SJ, Newsome PN, Weston CJ, Iredale JP, Tacke F, Pollard JW, Ponting CP, Marioni JC, Teichmann SA, Henderson NC. Resolving the fibrotic niche of human liver cirrhosis at single-cell level. *Nature* 2019;575:512–518.
31. Bodega B, Marasca F, Ranzani V, Cherubini A, Della Valle F, Neguembor MV, Wassef M, Zippo A, Lanzuolo C, Pagani M, Orlando V. A cytosolic Ezh1 isoform modulates a PRC2-Ezh1 epigenetic adaptive response in postmitotic cells. *Nat Struct Mol Biol* 2017;24:444–452.
32. Thabut D, Shah V. Intrahepatic angiogenesis and sinusoidal remodeling in chronic liver disease: new targets for the treatment of portal hypertension? *J Hepatol* 2010; 53:976–980.
33. Yaqoob U, Jagavelu K, Shergill U, de Assuncao T, Cao S, Shah VH. FGF21 promotes endothelial cell

- angiogenesis through a dynamin-2 and Rab5 dependent pathway. *PLoS One* 2014;9:e98130.
34. Min HK, Maruyama H, Jang BK, Shimada M, Mirshahi F, Ren S, Oh Y, Puri P, Sanyal AJ. Suppression of IGF binding protein-3 by palmitate promotes hepatic inflammatory responses. *FASEB J* 2016;30:4071–4082.
 35. Wang HH, Wang YC, Wu DW, Hung CS, Chen CY, Lee H. Targeting insulin-like growth factor-binding protein-3 by microRNA-125b promotes tumor invasion and poor outcomes in non-small-cell lung cancer. *Tumour Biol* 2017;39, 1010428317694316.
 36. Yang CH, Yue J, Pfeffer SR, Fan M, Paulus E, Hosni-Ahmed A, Sims M, Qayyum S, Davidoff AM, Handorf CR, Pfeffer LM. MicroRNA-21 promotes glioblastoma tumorigenesis by down-regulating insulin-like growth factor-binding protein-3 (IGFBP3). *J Biol Chem* 2014; 289:25079–25087.
 37. Chen L, Alexe G, Dharia NV, Ross L, Iniguez AB, Conway AS, Wang EJ, Veschi V, Lam N, Qi J, Gustafson WC, Nasholm N, Vazquez F, Weir BA, Cowley GS, Ali LD, Pantel S, Jiang G, Harrington WF, Lee Y, Goodale A, Lubonja R, Krill-Burger JM, Meyers RM, Tsherniak A, Root DE, Bradner JE, Golub TR, Roberts CW, Hahn WC, Weiss WA, Thiele CJ, Stegmaier K. CRISPR-Cas9 screen reveals a MYCN-amplified neuroblastoma dependency on EZH2. *J Clin Invest* 2018;128:446–462.
 38. Grzmil M, Hemmerlein B, Thelen P, Schweyer S, Burfeind P. Blockade of the type I IGF receptor expression in human prostate cancer cells inhibits proliferation and invasion, up-regulates IGF binding protein-3, and suppresses MMP-2 expression. *J Pathol* 2004;202:50–59.
 39. Conover CA, Bale LK, Durham SK, Powell DR. Insulin-like growth factor (IGF) binding protein-3 potentiation of IGF action is mediated through the phosphatidylinositol-3-kinase pathway and is associated with alteration in protein kinase B/AKT sensitivity. *Endocrinology* 2000; 141:3098–3103.
 40. Saldana SM, Lee HH, Lowery FJ, Khotskaya YB, Xia W, Zhang C, Chang SS, Chou CK, Steeg PS, Yu D, Hung MC. Inhibition of type I insulin-like growth factor receptor signaling attenuates the development of breast cancer brain metastasis. *PLoS One* 2013;8:e73406.
 41. Ricort JM, Binoux M. Insulin-like growth factor-binding protein-3 activates a phosphotyrosine phosphatase. Effects on the insulin-like growth factor signaling pathway. *J Biol Chem* 2002;277:19448–19454.
 42. Valenti L, Fracanzani AL, Bugianesi E, Dongiovanni P, Galmozzi E, Vanni E, Canavesi E, Lattuada E, Roviato G, Marchesini G, Fargion S. HFE genotype, parenchymal iron accumulation, and liver fibrosis in patients with nonalcoholic fatty liver disease. *Gastroenterology* 2010; 138:905–912.
 43. Kowdley KV, Belt P, Wilson LA, Yeh MM, Neuschwander-Tetri BA, Chalasani N, Sanyal AJ, Nelson JE; NASH Clinical Research Network. Serum ferritin is an independent predictor of histologic severity and advanced fibrosis in patients with nonalcoholic fatty liver disease. *Hepatology* 2012;55:77–85.
 44. Cabantchik ZI. Labile iron in cells and body fluids: physiology, pathology, and pharmacology. *Front Pharmacol* 2014;5:45.
 45. Huq A, Singh B, Meeker T, Mascarenhas D. The metal-binding domain of IGFBP-3 selectively delivers therapeutic molecules into cancer cells. *Anticancer Drugs* 2009;20:21–31.
 46. Polyzos SA, Perakakis N, Boutari C, Kountouras J, Ghaly W, Anastasilakis AD, Karagiannis A, Mantzoros CS. Targeted analysis of three hormonal systems identifies molecules associated with the presence and severity of NAFLD. *J Clin Endocrinol Metab* 2020;105:e390–e400.
 47. Yang L, Kwon J, Popov Y, Gajdos GB, Ordog T, Brekken RA, Mukhopadhyay D, Schuppan D, Bi Y, Simonetto D, Shah VH. Vascular endothelial growth factor promotes fibrosis resolution and repair in mice. *Gastroenterology* 2014;146:1339–1350 e1.
 48. Simonetto DA, Yang HY, Yin M, de Assuncao TM, Kwon JH, Hilscher M, Pan S, Yang L, Bi Y, Beyder A, Cao S, Simari RD, Ehman R, Kamath PS, Shah VH. Chronic passive venous congestion drives hepatic fibrogenesis via sinusoidal thrombosis and mechanical forces. *Hepatology* 2015;61:648–659.
-
- Received October 30, 2019. Accepted May 14, 2020.**
- Correspondence**
 Address correspondence to: Vijay H. Shah, MD, or Sheng Cao, MD, Gastroenterology Research Unit, Division of Gastroenterology and Hepatology, Mayo Clinic and Foundation, 200 First Street SW, Rochester, Minnesota 55905. e-mail: shah.vijay@mayo.edu or Cao.Sheng@mayo.edu; fax: (507) 255-6318.
- CRedit Authorship Contributions**
 Usman Yaqoob (Formal analysis: Lead; Methodology: Lead; Writing – original draft: Lead; Writing – review & editing: Equal); Fanghong Luo (Formal analysis: Equal; Methodology: Equal; Conceived and designed research; performed experiments: Equal); Thomas Greuter (Formal analysis: Supporting; Methodology: Supporting; Writing – review & editing: Supporting; Performed experiments: Supporting); Nidhi Jalan Sakrikar (Methodology: Supporting); Tejasav S Sehwat (Formal analysis: Supporting; Methodology: Supporting); Jianwen Lu (Formal analysis: Supporting; Methodology: Supporting); Xiao Hu (Formal analysis: Supporting; Methodology: Supporting); Jinhang Gao (Formal analysis: Supporting; Methodology: Supporting); Enis Kostallari (Formal analysis: Supporting; Methodology: Supporting); Jingbiao Chen (Formal analysis: Supporting; Methodology: Supporting); Juan P Arab (Formal analysis: Supporting; Methodology: Supporting); Sheng Cao (Formal analysis: Supporting; Methodology: Supporting; Writing – review & editing: Equal); Vijay H Shah, M. D. (Conceptualization: Lead; Project administration: Lead; Supervision: Lead; Writing – review & editing: Lead).
- Conflicts of interest**
 The authors disclose no conflicts.
- Funding**
 This study was supported by the National Institutes of Health grants DK59615 and AA021171 (V.H.S.); Clinical Core of the Mayo Clinic Center for Cell Signaling in Gastroenterology grant P30DK084567 (N.F.L.); National Natural Science Foundation of China grant 81472458 (F.L.); Fujian Natural Science Foundation grant 2017R1036-3 (F.L.); and Swiss National Science Foundation grant P2ZHP3_168561 (T.G.).